Available online at www.sciencedirect.com
SCIENCE DIRECT®
Applied Surface Science 247 (2005) 590–601
applied surface science
www.elsevier.com/locate/apsusc

Laser manipulation of clusters, structural defects and nanoaggregates in barrier structures on silicon and binary semi-conductors

G.I. Vorobets *, O.I. Vorobets, V.N. Strebegev

Yu. Fedkovych Chernivtsi National University, Faculty of Computer Science 2, Kotsyubynskoho Str., 58012 Chernivtsi, Ukraine

Available online 11 April 2005

Abstract

The methods of optical and scanning electron microscopy (SEM) along with electronic probe X-ray spectral microanalysis proved an opportunity to manipulate by means of laser irradiation with clusters, structural impurity defects and nanoaggregates in a space charge region (SCR) of a semiconductor in devices with a Schottky barrier formed on the basis of silicon and chalcogenide semiconductors. The optimal conditions of intensity of the millisecond laser irradiation at which the sizes of clusters diminish considerably are established, as well as the densities of edge dislocations in SCR and of dot defects. The dependences of the surface states density on contact, of the density of the deep levels in SCR and transition nanosize layer on a metal–semiconductor contact on the conditions of a laser exposure are studied. The presence of both the 5/500 nm deep transition structured layer and the modulated band gap causes the occurrence of tunnel-resonance charge transfer in contacts with a Schottky barrier, which can result in the appearance of sites with negative differential resistance in a current–voltage characteristic of the investigated structures.

Keywords: Semi-conductors; Laser; Schottky barrier; Structural defects

1. Introduction

The rapid progress in modern digital optical-electronic telecommunication control systems and networks is to the considerable extent caused by development of barrier structures on silicon, as well as on binary and ternary semiconductor compounds. Thermovision imaging systems not only utilize technologically well studied materials, such as Si, InSb, CdSb, $Hg_{1-x}Cd_xTe$, but also use visible and IR detectors, tuneable injected lasers, adsorptive optical filters, including Schottky diodes (DS), manufactured on the basis of the solid solutions of $Pb_{1-x}Sn_xTe$, $Pb_{1-x}Sn_xSe$ and InSe [1,2].

The methods of p–n-junction and heterostructure formation with the use of liquid-phase recrystallization

* Corresponding author. Tel.: +38 372 55 58 96/24 68 77; fax: +38 372 55 29 14.
E-mail address: vgeorge@au.cv.ua (G.I. Vorobets).

0169-4332/$ – see front matter © 2005 Elsevier B.V. All rights reserved.
doi:10.1016/j.apsusc.2005.01.081

of a surface of a semiconductor at the exposure to pulse laser irradiation (PLI) are properly investigated [3–7]. However, if the PLI treatment technique of silicon structures does not cause some difficulties, the one of semiconductor compounds is characterized by several peculiarities. Depending on such PLI conditions, as output intensity I_0, pulse duration t, temperature of semiconductor T and state of its surface, namely reflectivity R, not only diffusive redistribution of impurities and formation of non-equilibrium solid solutions becomes possible, but also considerable transpiration of atoms of some chemical elements from the treated area. This process is accompanied by deterioration of stoichiometric composition of the irradiated compounds, which is rather difficult to monitor. To rule out the mentioned shortcuts caused by PLI one should utilize the modes of metal–semiconductor (MES) contact treatment, which ensure the occurrence of inter-phase interaction in vicinity of the interface of MES in solid phase. Thus, as it was shown in [8,9], it provides an effective control over redistribution of structural impurity defects, and consequently, over the operating parameters of DS.

The purpose of the present work was to study experimentally physical mechanism of laser manipulation with structural impurity imperfections and nanoaggregates in a space charge region (SCR) of MES, where interaction of semiconductor with metal can lead to formation of solid solutions, silicides and other chemical compounds, in various structural modifications, as well as to consider the possibility of PLI application to a photon correction of physical properties of barrier structures.

2. Experimental technique

In order to carry out a study of physicochemical processes on the inter-phase interfaces of MES we considered four systems of contacts of Al–Si, Pt–Si, Al(Au)–PbTe($Pb_{1-x}Sn_xTe$) and Al(Au)–In_4Se_3, respectively, known to differ in their physical properties.

In the Al–Si system metal does not chemically interact with semiconductor. At isothermal annealing or PLI the formation of the Si:Al solid solutions turns out to be the possible [8,9]. On the contrary, the high-temperature treatment of the Pt–Si structures promotes formation of the Pt_2Si, PtSi and $PtSi_2$ silicides, depending on the duration of the process and its temperature mode [10].

The solid solution of $Pb_{1-x}Sn_xTe$ can be considered as two face-centred sublattices (anionic: Te and cationic: Pb and Sn), shifted by a (1/2, 1/2 and 1/2) vector [11,12]. According to X-ray diffraction the initial sample showed the atoms of metal to settle down statistically. Unlike the silicon structures, the presence of imperfections or slight deviation from stoichiometry, resulting from PLI in the given system, can lead to semiconductor band gap width alteration. As the result, formation of heterojunction becomes possible, and consequently, one should expect the change in physical properties of a barrier.

The phase diagrams of the In–Se system prove several structural modifications of semiconductor compounds of In_xSe_y: In_2Se (In_4Se_3), InSe, In_5Se_6 (In_6Se_7), In_5Se_7 and In_2Se_3 to be formed at different temperatures [11]. To our mind, the origin of the considerable temperature gradients and thermoelastic tensions in sub-contact area of the structures of metal—In_xSe_y exposed to PLI can promote phase transitions of the material from one structural modification to another.

The semiconductor crystals were prepared by conventional technique [9,12]. The metal contacts were manufactured with the help of magnetron or thermal evaporation of metal (Pt and Al) in vacuum. To shape the pattern of plating in silicon structures photoengraving was used, while for chalcogenides deposition through metal masks and chemical deposition of Au from water solution of $H[AuCl_4]\cdot 4H_2O$ was utilized.

The physical structure of the metallic foil, transition layer and contact layers of a semiconductor was investigated by means of optical and scanning electron microscopy, electron diffraction and small-angle X-ray diffraction. To detect the microstructure of aluminium the HF:HCl:H_2O etcher was used. The microstructure of silicide was studied with the help of the H_2O_2 + H_2SO_4 etcher, while for imperfection detection in subsurface layer of silicon of DS of Al–Si, Pt–Si the selective chromic etcher of CrO_3:H_2O:HF was used. The change in depth of transition layer in Si was estimated from time dependencies of current of an electroetching of plates–satellites [8]. The profiles of distributions of electrically active impurity in subsurface layers of a semiconductor were calculated from the (C–V) characteristics of the DS.

Yttrium–aluminium garnet in free-running mode with the radiation wavelength $\lambda = 1.06\ \mu m$ was utilized as a PLI source. The DS underwent the impact of single pulses of millisecond duration. The intensity I_0 of radiated energy ranged from 10 kW/cm^2 to 20 MW/cm^2, by means voltage variation applied to the active element of the pump, ray defocusing and diaphragm.

Real temperature $T(r, x, t)$ of the MES surface ($x = 0$) heated under PLI was estimated theoretically (Fig. 1a) on the basis of the results of experimental simulation (Fig. 1b and c) of thermal radiation effect on structures of Al-n-Si, utilizing a semiempirical relationship [3,8]:

$$T(r,0,t) = \left[\frac{(1-R)I_0 d}{K\pi^{1/2}}\right] \operatorname{arctg}\left(\frac{4æt}{d^2}\right)^{1/2} \exp\left(\frac{-r^2}{d^2}\right); \quad (1)$$

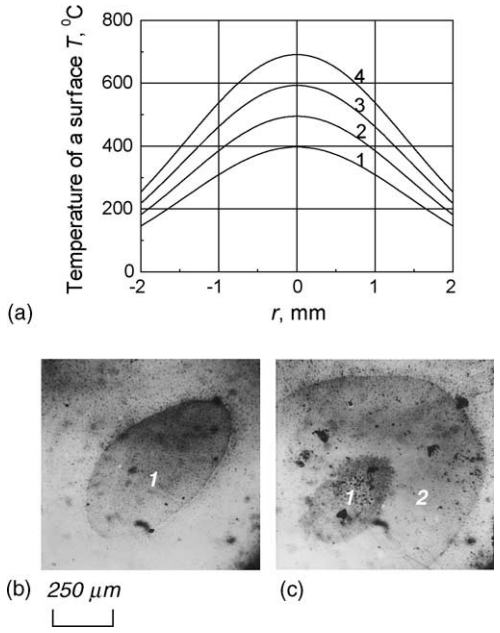

Fig. 1. Theoretical (a) and experimental (b and c) simulation of a radial distribution of temperature on the MES interface at PLI of the Al-n-Si structures: (a) radial distribution of temperature in MES at intensity of PLI $I_0 = 65$ kW/cm^2 (1), $I_0 = 85$ kW/cm^2 (2); $I_0 = 105$ kW/cm^2 (3) and $I_0 = 135$ kW/cm^2 (4); (b) the image of modification of the Al–Si system, heated up to eutectic temperature ($T_e = 577$ °C) at $I_0 = 105$ kW/cm^2; (c) areas of a MES heating up to T_e (2) and melting temperature (1) of Al ($T_m = 660$ °C) at $I_0 = 135$ kW/cm^2.

where R is the reflectivity of the irradiated surface, d the Gaussian beam radius, K the heat conductivity coefficient, $æ$ is the coefficient of thermal conductivity of a crystal.

It was assumed, that in the given case PLI displays thermal effect [4,9]. First morphologically modified area was observed on the Al surface (Fig. 1b, area 1). It results from the warm-up temperature of the surface, approaching the eutectic point of the Al–Si system ($T_e = 577$ °C) at the centre of a spot formed by incident ray on the interface of the system. The appearance of another modified area (Fig. 1c, area 1) is related to achievement of melting point of aluminium film ($T_m = 660$ °C).

3. Experimental results and discussion

3.1. Kinetics of defects and diffusion processes in the Al–Si system

Metallographic survey of the morphology of the aluminium film surface for two groups of the Al–Si DS, one of which primarily to PLI was thermally treated at $T = 450$ °C, enabled us to define a threshold value of PLI intensity in the given structures equalling $I_c \approx 95$–105 kW/cm^2. At irradiation of structures in the modes where $I_0 < I_c$ no essential changes in morphology of Al surface were observed. The I_0 variation from 105–115 kW/cm^2 up to 125–135 kW/cm^2 increases the temperature at the centre of an irradiation spot approximately from 550–600 °C up to 650–750 °C. The central symmetry and homogeneity over the area of the generated regions (Fig. 1a) testifies to homogeneity of the transition layer on inter-phase interface of Al–Si. Noteworthy, that at an irradiation of the Al film of large area the change in morphology of metal occurs at the centre of a spot of the incident irradiation. At an irradiation of separate contacts at the same intensity of PLI, providing the diameter of a ray not to exceed a diameter of a contact, the Al film morphologically varies over the perimeter of the contact.

In sub-contact layers of Si after Al being etched the triangular pits, characteristic for (1 1 1) orientation of a plate stipulated by defects of a substrate are observed. The packaging defects and emergency of dislocation lines accumulation turned out to be

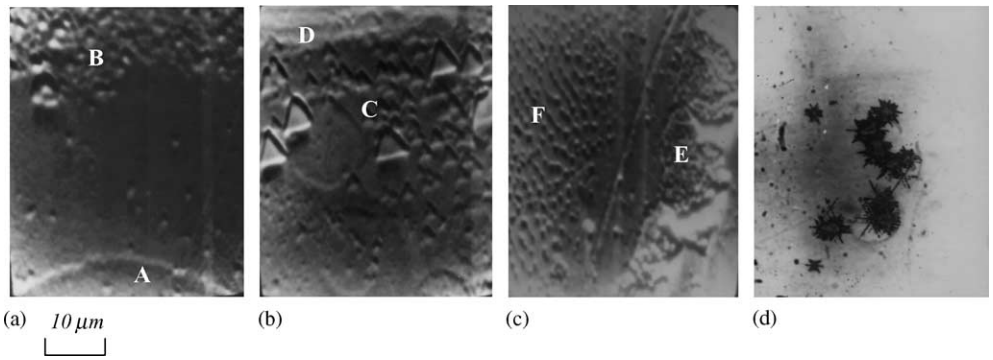

Fig. 2. Morphology of a silicon surface after pulse laser irradiation of Al-n-Si and etching of aluminium. (a) Forming of a defect system outside aluminium contact at $I_0 < I_c$; (A) silicon under a film of aluminium; (B) silicon outside Al-n-Si DS; (b) formation of structural defects under aluminium contact at $I_0 > I_c$; (C) defects under aluminium film, (D) the Al-n-Si interface; (c) formation of transition p^+-layer on the interface of Al-n-Si (area E) and system photostimulated defects in silicon outside the contact of Al-n-Si (site F) at $I_0 \approx I_c$ in the structures of Al-n-Si, thermally treated before PLI; (d) formation of crystallographically oriented defect systems on the irradiated surface of silicon at $I_0 \geq I_c$. (a–c) The SEM imaging, (d) the pattern obtained by metallographic microscope.

dominating. The increase in radiation intensity I_0 from 80 up to 95 kW/cm^2 results in complete vanishing of imperfections in sub-surface layers of Si under the Al film (Fig. 2a, site A) and formation of defect clusters along the perimeter of the contact beyond DS (Fig. 2a, site B) at the distance from 3–5 μm to 20–70 μm depending on a contacting area. At the intensity of PLI $I_0 > I_c$ the reverse process is yielded. The defects are accumulated inside the contact (Fig. 2b, C) at their complete absence beyond MES (Fig. 2b, D). The increase in I_0 up to 105 kW/cm^2 is accompanied by formation of continuous sponge-like defect layer on the interface of Al–Si under the Al film in the contacts not thermally treated. Considerable increase in transition of p^+-layer (Fig. 2c, E) [8] in thermally annealed structures is observed. The similar effect of PLI on silicon can lead to formation the arranged systems of photoinduced defects (Fig. 2c, F). It is necessary to stress, that, independently on preliminary thermal treatment at the mentioned PLI modes, the inter-phase interaction between Al and Si in the contact area occurs in a solid phase.

No changes in morphology of the Al surface in MES under irradiation through a silicon substrate were detected. The redistribution of a defect system over the effective area of Si arises at $I_0 \approx I_c$ as a separate chain of adjoining equilateral triangular pits along the perimeter of aluminium contact. However, when $I_0 > I_c$ a defect cluster (Fig. 2d) and yields of a grid of dislocation lines are clearly distinguished on the irradiated surface of silicon after chemical treatment. At $I_0 > 115$–120 kW/cm^2 the surface of Si(1 1 1) becomes amorphous or development of microcracks at 60° or 120° angle is observed [8,9] on the cleavage planes according to a crystallographic orientation of a chip.

Distribution of the impurities in SCR of the Al-n–n^+-Si–Al DS was estimated using the (C–V) results. The concentration of doping impurity in the initial crystal equals $n_0 \approx 2 \times 10^{16}$/cm^3, the corresponding magnitude of chemical potential for n-Si is $\mu = E_c - E_F \approx 0.19$ eV. Defined from linear approximation of the $1/C^2 = f(U)$ dependencies at direct bias, the magnitude of curving of energy bands φ_0 on the Al-n-Si interface for initial structures and for those after PLI at $I_0 = 85$ kW/cm^2 acquires values of 0.54 and 0.62 eV, respectively. These parameters are in good agreement with the relevant values of potential energy barrier $\varphi_b = \mu + \varphi_0 = 0.73 \pm 0.01$ eV and $\varphi_b = 0.81 \pm 0.01$ eV for the named DS, calculated from direct branches of the (I–V) characteristics. The analogous values of the barrier height, derived from linear approximating at reverse biases, yield a little overestimated values of $\varphi_b = 0.86 \pm 0.01$ and 0.88 ± 0.01 eV for the given structures.

The estimated thickness of transition p^+-layer by means of a direct (I–V) characteristic [9] at optimal modes of irradiation makes $l \approx 0.13$ μm. The magnitude is comparable to a shielding distance in a semiconductor at impurity concentration of $N_d = 10^{16}$/

cm^3. Thus, φ^* [9] rises up to 0.85 eV. The growth in φ_0 at $I_0 = I_c$ is explained satisfactorily by the appearance of p^+-layer and is compounded with corresponding data on thermal annealing. However, at heat treatment such process is accompanied by increase in ideality coefficient n up to 1.07, while at PLI the diminution of the same value down to 1.01 takes place.

The reverse (I–V) characteristic of irradiated at $I_0 = 85$ kW/cm^2 and unirradiated structures of the first group at small biases can be described by the $I_r \sim (U_r)^\beta$ relation with $\beta \approx 0.50$, being characteristic for generation current. The increase in I_0 up to I_c results in β diminution down to 0.20. Whereas, even at $I_0 = I_c$ some contacts at small voltages ($0 < U_r < 0.4$ V) can promote dependence, typical of generation current transition.

The correlation of the (I–V) (Fig. 3) and (C–V) characteristics with morphological changes observed in the Al-n-Si structure layers can be explained in terms of physical model, which takes into account thermoelastic tensions arising at the MES interface at PLI. At $I_0 < I_c$, thermoelastic compressions originating in the Al film, do not exceed its limit of elasticity. It favours the re-distribution of structural impurity defects in sub-surface layer of silicon and decrease in concentration of the deep levels, related to them, which are known to cause generation–recombination current in DS. In the mode of I_0–I_c, the activation of diffusive penetration of Al into Si in the field of elastic forces and increase in transition p^+-layer depth on the interface of MES are possible. The relaxation of thermoelastic tensions due to decomposition of the Al film at $I_0 > I_c$ brings about activation of the dissolution of Si in Al, and hence, leads to a increase in the concentration of defects on the interface of Al-n-Si. Thus, the density of levels on interface of Al-n-Si increases, causing more noticeable arise of the additional mechanisms of current transition in the given structures, and brings about the transformation of the rectifying (I–V) characteristics to the ohmic ones.

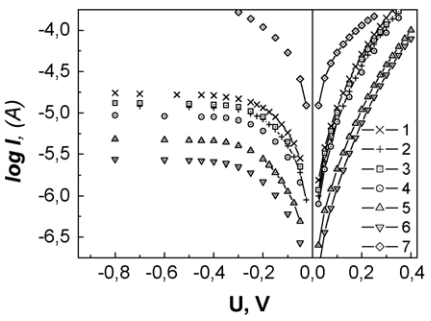

Fig. 3. The (I–V) characteristics of the Al-n-Si structures of the second group treated under different conditions of PLI: (1) $I_0 \approx 85$ kW/cm^2; (2) $I_0 \approx 95$ kW/cm^2; (3) $I_0 \approx 105$ kW/cm^2; (4) $I_0 \approx 113$ kW/cm^2; (5) $I_0 \approx 116$ kW/cm^2; (6) $I_0 \approx 117$ kW/cm^2; (7) $I_0 \approx 118$ kW/cm^2.

3.2. Silicide and imperfection re-structuring in the Pt–Si system

The PLI influence on the Pt_xSi_y–Si contacts was studied on two groups of the Al–Pt_xSi_y-n–n^+–p-Si DS, manufactured by a diffused planar process [13] and plates–satellites, relevant to them, with epitaxial n-Si layer on the p-Si substrate. The first group of the structures before being thermally annealed in nitrogen was additionally exposed to vacuum annealing during 10 min at $T = 480$ °C without opening the chamber after magnetronic deposition of platinum (thickness $h = 0.4$–0.6 μm). Contact area for one group ranged from 10 μm × 10 μm to 20 μm × 75 μm with diffusive p^+-guarding ring at the edges of the contact. While the contacts of another group were the same in area, but without p^+-ring.

The PLI treatment of Pt_xSi_y–Si contacts was carried out from the side of silicide under the conditions similar to those applied to the Al–Si structures.

Investigation of phase composition and crystallographic parameters of the structures, carried out by means of small angle X-ray diffraction and electron diffraction, indicated, that in the first group of contacts the continuous film of silicide in composition enriched by the PtSi phase was formed. The second group exhibited formation of polycrystallic film with the prevailing contributions of the Pt_2Si and $Pt_{12}Si_5$ phases. Increase in intensity up to $I_0 \leq I_c$ does not result in considerable changes in morphology of a silicide surface. But in both cases the irradiated film becomes more uniform and the reflexes of non-equilibrium phases appear to diminish in amplitude almost by the order. With $I_0 \approx 130$ kW/cm^2 at the centre of a spot on the surface of the first group of MES the periodic structures (Fig. 4a) are formed. The silicide is enriched by silicon and the emergency of both equilibrium phases of $PtSi_2$, and metastable

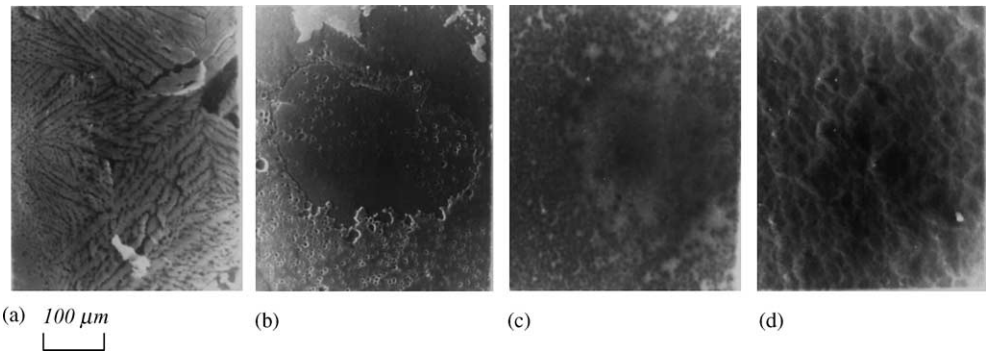

Fig. 4. Morphology of the silicide (a and c) and silicon (b and d) surfaces under the film of silicide after its etching obtained at PLI of the Pt_xSi_y-n-Si structures ($I_0 > I_c$). (a and b) Structures underwent high temperature treatment before PLI; (c and d) structure not preliminary treated. The image by SEM.

phases of Pt_2Si_3, Pt_4Si_9 should be expected. The second group film of silicide irradiated at the same PLI modes proves to be partially amorphous and contains the phases of PtSi and $PtSi_2$ (Fig. 4c).

The microscopic analysis of the silicon surface after complete etching of silicide proves the physical processes in structures of Pt_xSi_y–Si and Al–Si to be analogous at PLI. Irradiation intensity increases up to $I_0 \leq I_c$ with following drop in a density of imperfections in epi-Si under the layer of silicide at the centre of a spot in comparison with a periphery. The increase in defect concentration in epi-Si at $I_0 > I_c$, results in complete chemical interaction of a silicide film and epilayer of silicon, re-structuring the latter due to thermoelastic tensions and its removal at the etching a silicide (Fig. 4b). The microstructure of silicon surface of the second group of contacts after complete etching of silicide corresponds to enlargement of the grains of epi-Si over the irradiation area (Fig. 4d). This can be connected with transformation of the silicide crystallographic structure from tetragonal one for Pt_2Si to that typical of PtSi.

The electrophysical characteristics of the Pt_xSi_y-n-Si DSs strongly depend on preliminary vacuum annealing. The values of $\varphi_b = 0.80 \pm 0.01$ eV ($n = 1.03$) for the contacts with p^+-ring and $\varphi_b = 0.78 \pm 0.01$ eV ($n = 1.1$) for those without one, defined from the (I–V) characteristic for thermally treated DSs, agree well with a value of $\varphi_0 = 0.61$ eV ($\mu = 0.17$ eV), established in course of the (C–V) measurements. The contacts, which did not undergo additional treatment exhibited the corresponding parameters to equal $\varphi_b = 0.74 \pm 0.01$ and 0.72 ± 0.01 eV. The latter value of φ_b appears to be characteristic for the contacts of $PtAl_2$–Si [10].

PLI was found to enhance φ_b up to 0.86 ± 0.01 eV for the contacts with a guard ring and up to 0.81 ± 0.01 eV for those without it, where the saturation was achieved at the intensity of irradiation of $I_0 \approx I_c$. Ideality coefficient for these contacts decreases down to $n = 1.01$–1.03 and 1.06–1.08, respectively.

The transition over a maximum of the $n = f(I_0)$ dependency for the Pt_xSi_y-n-Si contacts is more likely to be related to the similar dependencies for the Al-n-Si contacts, when I_0 becomes lager than I_c. However, silicide dependency of the (I–V) characteristic parameters on the intensity of PLI is much narrower due to the difference in physicochemical processes occurring in the transition layer of the MES under PLI.

Strong influence of PLI is observed in the reverse (I–V) characteristic of the Pt_xSi_y-n-Si contacts. The increase in I_0 up to I_c leads to reduction of reverse currents for both groups of DSs by 1–2 orders of magnitude.

In DS of the second group the $\varphi_b = f(I_0)$ dependence does not show saturation at $I_0 = 95$–105 kW/cm^2. It linearly increases with the I_0 growth up to 115 kW/cm^2 both for the diodes without a guard ring (φ_b enlarges from 0.72 ± 0.01 eV up to 0.76 ± 0.01 eV, n linearly decreases from $n = 1.09$ to 1.04) and the diodes with p^+-ring (φ_b increases from 0.74 ± 0.01 eV up to $0.79 \pm 0{,}01$ eV, n diminishes from $n = 1.05$ to 1.02).

The occurrence of a generation–recombination current caused by deep levels, in the initial DS without a guard ring with respect to one with p^+-ring is displayed

as two linear sections of the (*I–V*) characteristic with different values of differential coefficient of linearity of $\alpha_1 = d(\ln I)/dV \approx 40$ at large biases ($V > V_0 = 0.45$–0.55 B) and of $\alpha_2 \approx 27$ at small ones ($V < V_0$) in the 270–290 temperature range. The increase in I_0 up to I_c reduces the temperature of additional current transport development by $\Delta T = 50$–70 K. In order to define activation energy E_t of deep levels temperature dependencies of $\log I = f(1/T)$ were utilized. In the field of low temperatures at different values of a forward bias levels are basically assigned to platinum, oxygen and point defects [14] with energies of -0.24 ± 0.02, 0.31 ± 0.02, 0.34 ± 0.02, 0.44 ± 0.02 and 0.47 ± 0.02 eV at small biases ($V < V_0$). A value of $E_a = 0.73 \pm 0.02$ eV (at $V > V_0$) corresponds to a value of potential energy barrier height for thermoemission mechanism of current transition. The effect of PLI on the contacts in the modes mentioned above causes annealing of deep centres with lower activation energy and more stable appearance of the level with $E_a = 0.46 \pm 0.02$ eV at all biases. At $V > V_0$, as well as before PLI, the value of activation energy agrees with a value of height of potential energy barrier of $E_a = \varphi_b = 0.77 \pm 0.02$ eV for over-barrier current.

On the basis of the obtained experimental data it is possible to conclude, that under PLI of the Al–Pt_xSi_y-n–n^+–p-Si contacts the electrical activity of the centres, causing additional currents, connected with the deep levels of platinum, impurities and structural imperfections in silicon, reduces.

3.3. Phase changes on a metal–In_4Se_3 interface

The phase modification of In_4Se_3 indium selenide crystallizes within a very narrow temperature band at a certain ratio of weight coefficients of the components. The compounds of InSe and In_2Se_3 are known to be more stable. They melt congruently at the temperatures of 660 and 900 °C, respectively. The phases of In_2Se and In_5Se_6 are generated due to peritectic reactions and melt at 540 and 660 °C, respectively. The given compounds possess trimetric structure and are semiconductor described by a covalent bonding inside each layer and by a feeble Van der Vaals one between layers. Each atom of Se inside a monolayer has three proximate neighbours, forming thus a hexagon unit cell [15,16]. Thus, originating at PLI the thermoelastic tensions on the interface of Al–In_4Se_3 can be described by translation vectors for a hexagonal unit cell. If the boundaries of grains of a polycrystalline film of Al coincide with translation vectors of the cell, they are prevailing directions of diffusion of chalcogenide or metal in a film of aluminium.

In Fig. 5a–c, different stages of interphase interaction in a system of Al–In_4Se_3 are shown depending on intensity of PLI: at $I_0 = 15$–20 kW/cm^2 (the Fig. 5a) diffusion of atoms of a substrate over tripled points of grains of aluminium is activated; at $I_0 = 20$–25 kW/cm^2 the one over aluminium grain boarder is observed (Fig. 5b); at $I_0 = 25$–35 kW/cm^2 (Fig. 5c, d) re-structuring of semiconductors, assuming due to change in phase composition in comparison with the one of starting material, is detected.

The metallurgical studies of a surface of the Au–In_4Se_3 contact after PLI of similar intensity display, that the critical values of I_0 for MES, formed by a method of chemical deposition from water solution are much higher in comparison with those obtained after evaporation. Apparently, it is caused by

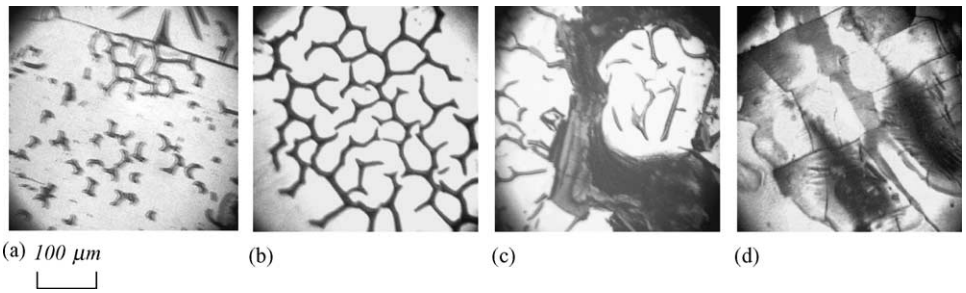

Fig. 5. Morphology of the metal contact surface in the Al-n-In_4Se_3 (a–c) structures and of the In_4Se_3 crystal (d) after PLI at different intensites: (a) $I_0 \approx 15/20$ kW/cm^2; (b) $I_0 \approx 20/25$ kW/cm^2; (c, d) $I_0 \approx 25/35$ kW/cm^2. The image by a metallographic microscope.

intercalation of atoms of gold to interplanar space of selenide and formation on the interface of Au–In_4Se_3 of a transition layer of the greater thickness, which at PLI damps development of elastic stresses in structure.

PLI of the In_4Se_3 crystals at intensity of $I_0 = 25$–35 kW/cm^2 results in phase re-structuring of a semiconductor (Fig. 5d), which is accompanied by change in type of electric conductivity of the irradiated surface. Further increase in I_0 may lead to delamination of a semiconductor substrate, due to occurrence of thermoelastic tensions exceeding the limit of elasticity of a crystal. Thus, structural modification of a crystal can be implemented both in solid and liquid phases depending on a heating temperature of the crystal.

The Au-n-In_4Se_3 barrier structures formed on a cleave of a basic crystal of n-type conductivity with impurity concentration of $n \approx (2/8) \times 10^{14}$/cm^3 [16], possess better detector properties (Fig. 6) in comparison with the similar structures of Al-n-In_4Se_3 formed on the same crystal. However, it's difficult to approximate the (*I*–*V*) characteristic of the given structures by the relations used for Schottky barriers, since the currents appear to be considerably restricted by serial resistance of the base of the diode. According to theoretical estimations, along with a thermoemission current the generation–recombination one is also shown to play a major part. The increase in the intensity of PLI up to the values of about 20–25 kW/cm^2 is resulted in gradual transformation of the (*I*–V) characteristic from the rectifying ones to those ohmic [7,17].

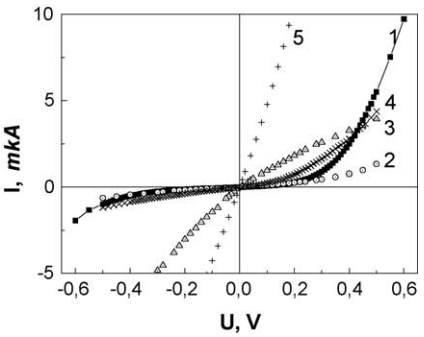

Fig. 6. The (*I*–*V*) characteristics of the Au-n-In_4Se_3 structures after PLI of different conditions: (1) film contacts of Au-n-In_4Se_3 before PLI; (2) dot pinch contact of Au-n-In_4Se_3 before PLI; (3) dot pinch contact to the irradiated area of In_4Se_3; (4 and 5) film contacts of Au-n-In_4Se_3 after PLI of $I_0 = 20$ and $I_0 = 35$ kW/cm^2, respectively.

3.4. Interphase interaction in a metal–$Pb_{1-x}Sn_xTe$ and metal–PbTe system

The composition of a surface of a ternary solid solution of $Pb_{1-x}Sn_xTe$ strongly depends on a chemical and mechanical polishing of the initial substrate carried out via the technique [8,11] in a solution of $K_3[Fe(CN)_6]$. The morphology of a surface has a relief character (Fig. 7a), which is preserved at deposition of an aluminium film. The thickness of the relief layer fall within the range from hundreds angstroms up to unit of nanometers. The critical values of intensity of PLI at an irradiation of structures of Al (Au)–PbTe and Al (Au)–$Pb_{1-x}Sn_xTe$ are much lower than those for silicon DS. Depending on the thickness of a metal film and the quality of surface treatment of the crystal they range within $I_0 \approx 20$–50 kW/cm^2. The character of interphase interaction between film of Al and the substrate of $Pb_{1-x}Sn_xTe$ is similar to the process of solid-state epitaxy in the systems of Al–Si and In_4Se_3 at isothermal annealing and PLI. As one can see from Fig. 7, at $I_0 \approx I_c$ the process of mutual diffusion of a semi-conductor and metal film through the crystal boundaries arises. However, in this case, unlike the previous one, the governing role is played by structuring of a substrate, not that of film. Further increase in intensity leads to the re-structuring of surface layer of $Pb_{1-x}Sn_xTe$ with enlargement of grain sizes and reduction of non-uniformity of a substrate surface (Fig. 7b) is observed.

The same intensities of PLI of Al contacts on PbTe result in decomposition of a metal film. That, apparently, is due to poor adhesion of plating to a substrate, which probably contained an oxide layer on its surface before deposition. The change in stoichiometry of sub-surface area of the given materials can be caused by the difference in formation energies of oxide phases in the systems of Pb–Te–O and Sn–Te–O [11]. In this case after the formation of crystallographically oriented grids of dislocations and pitches (Fig. 7d) on the crystal surface, exposed to PLI, is apparently predetermined by thermoelastic tensions.

Chemically deposited contacts of Au on a surface of PbTe and $Pb_{1-x}Sn_xTe$ show somewhat higher critical values of I_0 than those of Al. The phenomenon seems to be explained by formation of transition layer

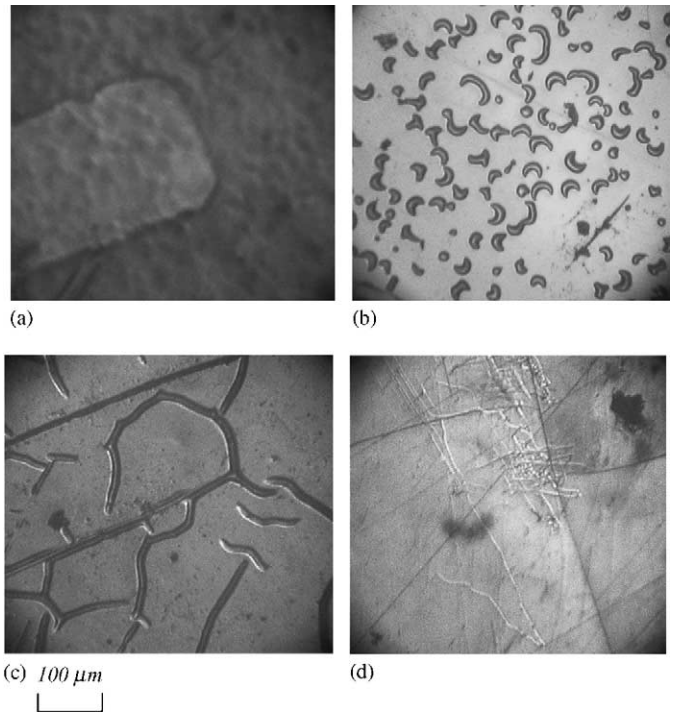

Fig. 7. Surface morphology of the Al-p-$Pb_{1-x}Sn_xTe$ structures (a–d) after PLI at different conditions: (a) surface of a film of Al (light area) and $Pb_{1-x}Sn_xTe$ (dark area) before PLI; (b) surface of the Al film after PLI at $I = 20$ kW/cm^2; (c) fracture of the Al film and development of microcracks on a substrate of $Pb_{1-x}Sn_xTe$ at $I_0 > I_c$; (d) grid of dislocations on a surface PbTe under a film Al, formed at $I_0 \approx I_c$.

due to substitutional reaction of metals in course of interaction between $Pb_{1-x}Sn_xTe$ and the $H[AuCl_4]$ solution. Thus, both in initial crystals and the Au–PbTe contacts after PLI treatment display granular surface.

The solid solutions of $Pb_{1-x}Sn_xTe$, PbTe and SnTe are known to solidify in the NaCl structure. They possess similar values of stationary lattice constants ($\alpha_{PbTe} = 6.46$ Å, $\alpha_{SnTe} = 6.327$ Å and $\alpha_{Pb0.8Sn0.2Te} = 6.4321$ Å) [12]. The area of primary crystallization of ternary compound of $Pb_{1-x}Sn_xTe$ borders on the area of extraction from the melt of the Pb–Te and Sn–Te solid solutions. In order to perform liquid phase epitaxy, the solution should be removed from the zone of epitaxy layer growth. Hence, implementation of liquid phase laser epitaxy may lead to separation of the crystals with phase composition different in a magnitude of E_g. It is possible to expect, that the presence of considerable thermoelastic compression in MES at PLI will also reduce the relevant re-structuring of the given system in a solid phase.

The identification of the process of re-structuring can be performed using, both the results of X-ray crystal analysis, and the electrophysical measurements of a band gap width of the semiconductor ($E_{gPbTe} = 0.318$ eV, $E_{gSnTe} = 0.18$ eV and $E_{gPb0.8Sn0.2Te} = 0.2$ eV at $T = 300$ K). Besides, when considerable deviation from stoichiometry, caused mainly by defects and by presence of vacancies of metal, occurs in crystals of $Pb_{1-x}Sn_xTe$, the anomaly of physical properties of a material explained by aspiration $E_g \rightarrow 0$ is observed.

The energies of vacancy formation in PbTe, defined from Coster–Slater model for localized potential and cluster calculations of the levels of imperfections in PbTe and SnTe, make $\varepsilon_{\upsilon Pb} = 0.3$ eV, $\varepsilon_{\upsilon Te} = 1.2$ eV) [12]. The aluminium is a donor, which, presumably, substitutes Pb in a lattice of PbTe. Therefore, at solid-state laser epitaxy on the interface of Al-p-PbTe one should expect the formation of nanodementional compensated layer and, accordingly, the Al-p^-–p-PbTe transition. The doping of $Pb_{1-x}Sn_xTe$ with aluminium, as well as with In, Ga, Cd results in the

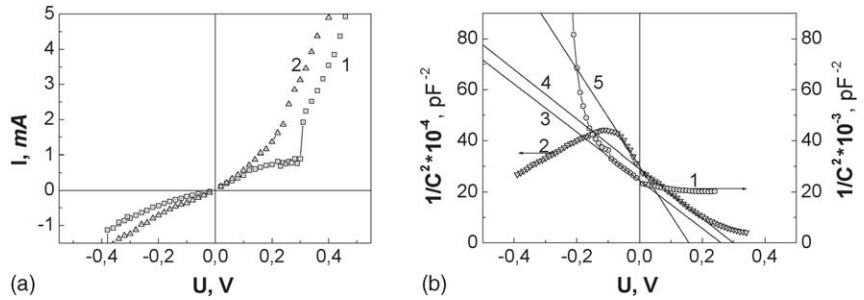

Fig. 8. Typical (I–V) characteristics (a) of the Al-p-$Pb_{1-x}Sn_xTe$ structures before and after PLI at $I_0 \approx 20$ kW/cm^2, and the $1/C^2 = f(U)$ dependencies (b) for the structures of Au-p-PbTe (1) and Al-p-PbTe (2), respectively; (3–5) theoretical interpolation of linear sections of the $1/C^2 = f(U)$ dependencies.

phenomenon of long-time relaxation of conductivity (LTR) [2,18,19], what is experimentally observed in the static (I–V) characteristic measurements of the investigated structures of $Pb_{1-x}Sn_xTe$ in shape of oscillating regions with negative differential resistance (Fig. 8a).

The analysis of the $1/C^2 = f(U)$ dependencies for the Al-p-PbTe and Au-p-PbTe DS (the Fig. 8b) displays, that structure of the transition layer on a metal–semiconductor is determined by technological features of MES formation. Taking into account a course of the $1/C^2 = f(U)$ dependency at reverse biases of $-0.4B < U < -0.2B$ (Fig. 8b, the line 2), it is possible to assume, that on a surface of the p-PbTe crystal before contact formation there was a thin tunnel oxide layer. Therefore, nanosize transition layer formed on the interface in course of aluminium deposition contains considerable amount of surface electron states. They create shallow levels in space-charge region of a semi-conductor and at once are ionized at direct biases applied to the junction. However, it brings about sufficient curving of the bands in SCR, the value of which found from approximation of a linear sections of the $1/C^2 = f(U)$ dependency at positive biases (Fig. 8b, the line 4), makes $\varphi_0 = 0.29 \pm 0.01$ eV for carrier concentration of $p = 2 \times 10^{18}$/cm^3 in the initial crystal. The value of $\varphi_0 = 0.16 \pm 0.01$ eV, determined from the beginning of the named dependency at reverse biases (Fig. 8b, 5), can point out the presence of a deep level (or even subzone) with a similar ionization energy in a space-charge region or dielectric layer between metal and semiconductor. Hence, a generation current is found to be a governing transport mechanism in the Al-p-PbTe structures at reverse biases.

The Au-p-PbTe structures also show the formation of the transition layer with a constant value of charge carrier concentration, ensuring $\varphi_0 = 0.26 \pm 0.01$ eV (Fig. 8b, 3). However, the (C–V) characteristics (Fig. 8b, 1) point out the formation of sharp p–n junction than that of DS barrier.

PLI of the Al(Au)–PbTe, Al(Au)–$Pb_{1-x}Sn_xTe$:Se structures at the optimal conditions appear to reduce considerably the surface state density and that of deep levels in the transition layer between metal and semiconductor. It provides diminution of the contribution of padding mechanisms current transport into over-barrier current and can presumably rule out the effect of long-time relaxation of conductivity (Fig. 8a, 2). Unlike the silicon structures the range of optimal conditions for this case is much narrower, which demands a precise control of laser irradiation intensity.

4. Conclusions

The experimental results of the investigations of physical mechanisms of laser manipulation with structural impurity defects and phase states of semiconductor compounds on metal–semi-conductor interface at PLI of barrier structures on silicon and chalcogenide semi-conductors allow one to make the following conclusions.

In the Al–Si structures, PLI results in occurrence of considerable temperature gradients and thermoelastic tensions in SCR of DS. It can intensify non-equilibrium diffusion processes in a solid phase,

which lead to formation of transition layer of inverse conductivity on the interface of MES and/or to redistribution of structural impurity defects in contact area of silicon. The presence of unambiguous correlation between irradiation intensity, redistribution of defects and parameters the (*I–V*) characteristic of DS of Al–Si makes PLI an efficient tool for a photon correction of parameters of barrier structures on silicon.

The optimal conditions of PLI for the Pt_xSi_y-n-Si contacts with polycrystalline structure of silicide can cause transformations in phase composition of silicide with its enrichment by platinum and formation of equilibrium phases of PtSi, $PtSi_2$. Moreover, the contacts with single crystal structure of silicide experience considerable thermoelastic tensions, which are known to give rise to microplastic deformations in nanosize transition layers of silicide and silicon. The given processes reduce concentration of deep levels, assigned to platinum and structural defects in SCR of Pt_xSi_y-n-Si DS. They also are found to increase potential barrier energy of the MES. The (*I–V*) characteristics of the named DS approach the ideal ones due to decrease in generation–recombination component of current by the order of 1–2.

Thermoelastic tensions arising at PLI in the Al(Au)-n-In_4Se_3 contacts activate both-way diffusion of the elements on boundaries of metal grains, stimulating intercalation of the atoms of metal and impurities into the interplanar space of selenide. It leads to reordering of the structure of the transition layer in MES and to stabilization of physical properties and parameters of the Al(Au)-n-In_4Se_3 DS. At the critical value of PLI intensity the restructuring of the semiconductor with following changes in phase composition and conductivity, becomes possible in the sub-surface layer of selenide, which results in non-uniformity of the contacts and degradation of the rectifying DS (*I–V*) characteristics to the ohmic ones.

PLI of the Al(Au)–PbTe, Al(Au)–$Pb_{1-x}Sn_xTe$ systems at intensity of radiation less than a critical value stimulates diffusive penetration of the metal atoms into semiconductor, compensation of conductivity type of chalcogenide transition layer and restricts activity of the centres, which bring about long-time relaxation of conductivity in course of the static (*I–V*) measurements of the MES. The PLI intensity greater than a critical value leads to emergency of the dislocation grid in the sub-surface layer of PbTe, where processes of non-uniform penetration of metal via the boundaries of the solid solution grains is observed, causing degradation of the MES barrier.

Thus, utilizing optimal conditions of PLI influence on of barrier structures on silicon, binary and ternary semiconductors, when the inter-phase interaction at the interface of MES occurrs in a solid phase, it is possible to drive effectively redistribution of structural impurity defects, diffusion processes and change in phase composition of a semiconductor in SCR of MES, and consequently, to ensure a photon correction of parameters and characteristics of barrier structures.

References

[1] R.J. Keyes (Ed.), Optical and Infrared Detectors, Springer–Verlag, Heidelberg, 1985 (Radio i sv'az', Moscow, 1985, p. 110).
[2] A.V. Lyubchenko, Ye.A. Sal'kov, F.F. Sizov, Principal Physics of Semiconductor Infrared Photonics. The Modern Tendencies New Materials, Naukova dumka, Kiev, 1984.
[3] W.W. Duley, Laser Processing and Analysis of Materials, Plenum, New York, 1983 (Mir, Moscow, 1986, p. 109).
[4] I.B. Khaybullin, G.P. Smirnov, Fiz. Tech. Poluprovodn. 19 (1985) 4.
[5] Z.Yu. Gotra, Laser Methods in Microelectronics, Svit, L'viv, 1991, p. 92.
[6] K.D. Tovstyuk, G.V. Plyatsko, V.B. Orlets'kiy, T.R. Kiyiak, Yia.V. Bobits'kiy, Ukr. Fiz. Jurn. 21 (1976) 1918.
[7] Yia.V. Bobits'kiy, T.S. Gertovich, T.R. Kiyak, G.V. Plyatsko, K.D. Tovstyuk, Ukr. Fiz. Jurn. 23 (1978) 685.
[8] G.I. Vorobets, M.M. Vorobets, V.N. Strebeshev, E.V. Buzaneva, A.G. Skavro, Semiconductors 38 (2004) 663.
[9] G.I. Vorobets, O.I. Vorobets, A.P. Fedorenko, A.G. Skavro, Funct. Mater. 10 (2003) 468.
[10] S.P. Murarka, Silicides for VLSI Applications, in: Bell Telephone Laboratories, Murray Hill, New Jersey, 1983 (Mir, Moscow, 1986, p. 121).
[11] V.P. Zlomanov, A.V. Novosyiolova, P-T-x- of the Phase Diagram of Systems Metal—Chalcogen, Science, Moscow, 1987, p. 121.
[12] N.P. Gavaleshko, P.N. Gorley, V.A. Shenderovskiy, Narrow-Bandgap Semi-Conductors: Preparation and physical properties, Naukova dumka, Kiev, 1984, p.107.
[13] E.V. Buzaneva, G.I. Vorobets, O.V. Nikulin, V.I. Strikha, A.G. Shkavro, Electronic engineering. Series 2, Semicond. Devices 3 (200) (1989) 49.
[14] A.G. Milnes, Deep Impurities in Semiconductors, John Willey & Sons, New York, Sydney, Toronto, 1973 (Mir, Moscow, 1977, p.22).

[15] K.D. Tovstyuk, Semiconductor Material Science, Naukova dumka, Kiev, 1984, p.74.
[16] T.S. Gertovich, S.I. Griniova, B.N. Gritsyuk, A.D. Ogorodnik, O.T. Stolyarchuk, K.D. Tovstyiuk, Ukr. Fiz. Jurn. 27 (1982) 8.
[17] S.I. Drapak, V.B. Orlets'kiy, Z.D. Kovalyuk, V.V. Netyaga, Fiz. Tech. Poluprovodn. 37 (2003) 196 (Sov. Phys. Semicond.).
[18] L.A. Hemstreet, Phys. Rev. B 12 (1975) 1213.
[19] K. Weiser, Phys. Rev. B 23 (1981) 2741.